Real-time Voltage Control to Improve Automation and Quality in Power Distribution

FRANCESCO MUZI
Department of Electrical Engineering and Computer Science
University of L'Aquila
Piazzale Pontieri, 1 - L'Aquila 67100
ITALY
muzi@ing.univaq.it

Abstract: - A new power digital voltage controller is described able to improve quality in power distribution using real-time compensation of both slow voltage changes and quick disturbances as sags and swells. Voltage control was achieved by means of a special transformer able to change the magnetic flux linked to the secondary winding; moreover, secondary voltage was monitored through a feedback control managed by a properly programmed micro-controller. The completely automated system includes a power section, namely a special transformer, a power electronic section consisting of an inverter driven by an actuator, and a digital section involving a micro-controller with implemented software. The capabilities of the proposed voltage conditioner were verified by laboratory experimental tests performed on a specifically manufactured prototype. Experimental results are reported and the behavior of the conditioner under different working conditions is discussed.

Key-Words: - Electrical distribution systems, Power quality, Power systems control and automation, Voltage conditioning.

1 Introduction

The whole concept of voltage quality in power distribution has undergone great changes in the last few years [2], [4], [5], [6], [8], [9], [13], [14]. In the past only shifts from rated values used to be taken into account, whereas today a number of anomalies must be evaluated. These anomalies, commonly named disturbances, can be classified as follows:

- long interruptions;
- short interruptions;
- micro-interruptions;
- slow voltage changes;
- sags;
- swells;
- harmonics.

Disturbances depend on a number of events, of which the most important are:

- atmospheric phenomena such as wind, rain, snow, lightning, etc. [15];
- environmental conditions, mainly pollution;
- the diffusion of non linear loads causing harmonic distortion and voltage fluctuations.

The herein described voltage conditioner has the main aim to eliminate slow voltage changes, sags and swells [10], [11], [12], [17]. The suggested voltage controller was derived from a power conditioner proposed in the past by the same author [1], now properly modified to achieve better performance in voltage control, with changes in both the power-unit configuration and the previously adopted processing software.

The system is arranged in three main sub-systems, namely a power electric unit, a power electronic section and a digital electronic control, and completed with a specifically implemented processing software.

Voltage control is obtained without on-load tap changers by varying the magnetic flux linked to the secondary winding of a special transformer. A digital feedback control system performs a continuous on-line supervision of all subsystems involved, and enacts voltage conditioning whenever either slow or quick changes are detected. All control actions are achieved by means of a balancing inverter automatically activated by the control system.

2 System description and modeling

The complete layout of the new voltage controller is shown in Fig. 1.

The power unit is controlled by a micro-processor (μP) on the basis of information received from a Data Acquisition System (DAS). The μP drives a small inverter that, in its turn, works as an actuator. The rated power of the inverter is small when compared to that of the whole system. The power unit consists of a special transformer provided with a magnetic shunt able to deviate part of the flux generated by the primary winding, making it possible to control the magnetic flux linked to the secondary winding.

The working principle of the proposed transformer is shortly described in the following, assuming a single-phase machine for simplicity reasons. The special transformer has three legs and four windings placed around only two of the legs. Two windings, placed on the first and third legs, work as a balancing winding and a primary winding, respectively. The other two windings, also placed on the first and third legs, are connected serially forming a secondary winding.

Fig. 2 shows the layout of the new electrical machine.

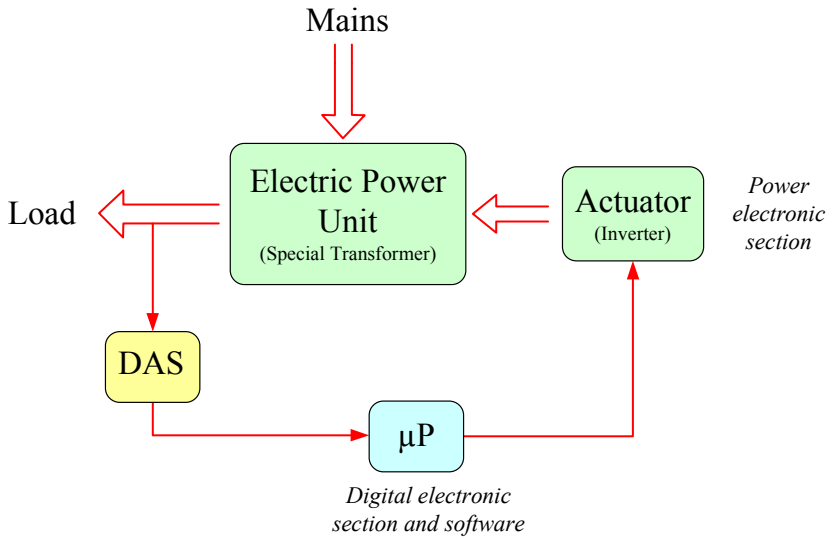

Fig.1 System layout.

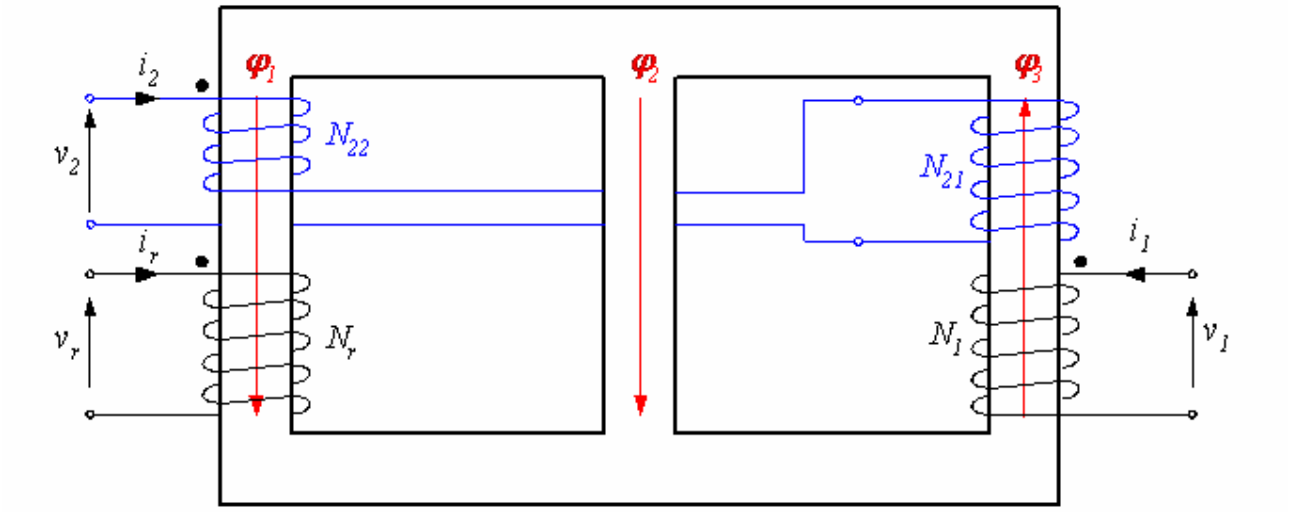

Fig.2 Layout of the power unit.

Fig. 2 also illustrates the conventional directions of both the currents and magnetic flux. The two N_{21} and N_{22} windings - together forming the secondary winding - must have same-phase electromotive forces. Assuming the electromotive forces of the N_{21} and N_{22} windings as e_{21} and e_{22}, respectively, the following relation can be written:

$$e_2 = e_{21} + e_{22}$$

In order to obtain good results, it is necessary to set the N_1/N_{21} ratio as equal to the nominal ratio. In addition, the number of coils in the N_r balancing winding must be established keeping in mind that any increase in their number implies a reduction in the magnetizing current. Finally, in order to reduce the power flow in the balancing winding, N_{22} must be much lower than N_{21}.

In order to better understand the behavior and capabilities of the proposed machine, an equivalent circuit must be defined so as to simulate the machine providing important indications for prototype design. In the first stages the proposed equivalent circuit involved an ideal transformer [3], but afterwards more precise models were built by adding a leakage flux as well as iron and copper losses.

The complete equivalent circuit of the special transformer is shown in Fig. 3, while the associated mathematical model is the following:

$$\dot{V}_1 = \left(R_1 + j\omega L_{\sigma 1}\right)\dot{I}_1 + \dot{E}_1 = \left(R_1 + jX_{\sigma 1}\right)\dot{I}_1 + \dot{E}_1$$

$$\dot{V}_r = \left(R_r + j\omega L_{\sigma r}\right)\dot{I}_r + \dot{E}_r = \left(R_r + jX_{\sigma r}\right)\dot{I}_r + \dot{E}_r$$

$$\dot{V}_2 = \left(R_2 + j\omega L_{\sigma 2}\right)\dot{I}_2 + \dot{E}_2 = \left(R_2 + jX_{\sigma 2}\right)\dot{I}_2 + \dot{E}_2$$

$$\dot{E}_1 = j\omega L_{\mu 1}\dot{I}_{\mu 1}$$

$$\dot{E}_r = j\omega L_{\mu r}\dot{I}_{\mu r}$$

$$\dot{E}_2 = \dot{E}_{21} + \dot{E}_{22} = \frac{N_{21}}{N_1}\dot{E}_1 + \frac{N_{22}}{N_r}\dot{E}_r$$

$$\dot{I}_1 = \dot{I}_{\mu 1} + \frac{\dot{E}_1}{R_{fe1}} + \dot{I}_1^{r} + \dot{I}''_{1,21} + \dot{I}''_{1,22} = \dot{I}_{\mu 1} + \dot{I}_{fe1} + k_{1r}\dot{I}_r + k_{1,21}\dot{I}_2 + k_{1,22}\dot{I}_2$$

$$\dot{I}_r = \dot{I}_{\mu r} + \frac{\dot{E}_r}{R_{fer}} + \dot{I}'_r + \dot{I}''_{r,22} + \dot{I}''_{r,21} = \dot{I}_{\mu r} + \dot{I}_{fer} + k_{r1}\dot{I}_1 + k_{r,22}\dot{I}_2 + k_{r,21}\dot{I}_2$$

The equivalent circuit of the special transformer shown in Fig. 3 was conveniently used to optimize the prototype design.

The prototype was further improved by reducing both the power necessary for voltage control actions, and the rated power of the inverter connected to the compensating coil. Once the prototype was built, a number of significant operating conditions were investigated.

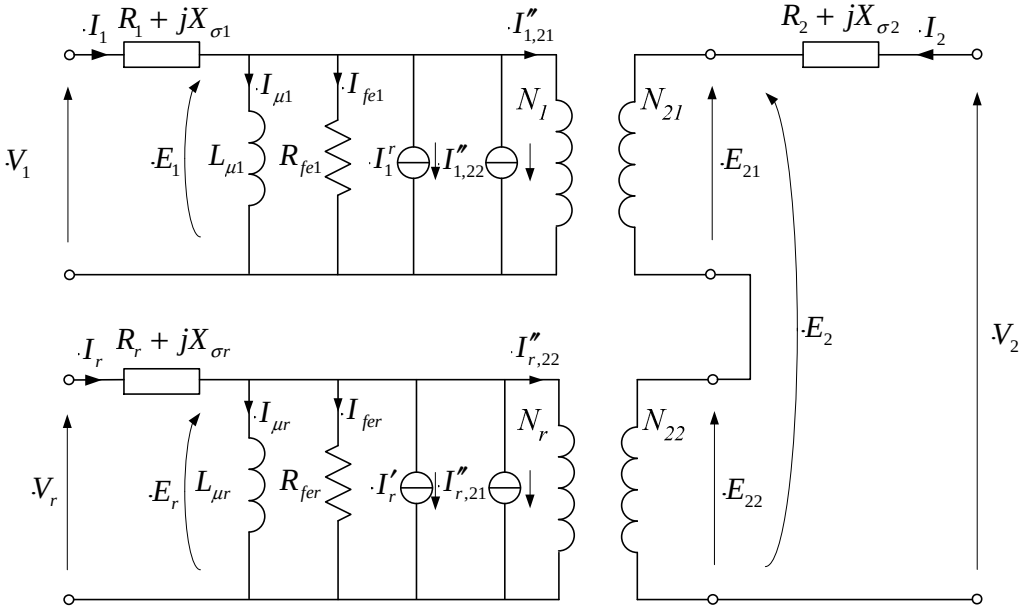

Fig.3 Equivalent circuit of the special transformer.

3 Evaluation of the parameters of the equivalent circuit

When the non-ideal parameters of a transformer are known, engineers can optimize design using equations rather than inefficiently wasting time in testing laboratory physical implementations, which means that designs could be optimized before any implementation took place.

With reference to the equivalent circuit of Fig. 3, the transformer parameters were evaluated by means of open circuit and short circuit laboratory tests performed directly on the built prototype.

3.1 Open circuit tests

Open circuit tests allow to calculate derived parameters as R_{fe1}, R_{fer}, $X_{\mu 1}$ e $X_{\mu r}$.

From specialized literature it is well known that an open circuit test is performed by applying rated voltage to the supplied circuit while leaving the other circuits open. Two tests were performed supplying either the primary or the compensation winding.

It is also well established that since under these conditions all series parameters and current generators can be neglected, only the values of parallel parameters need to be evaluated. As concerns the two open circuit tests, the equivalent circuits adopted are shown in Figs. 4 and 5, respectively.

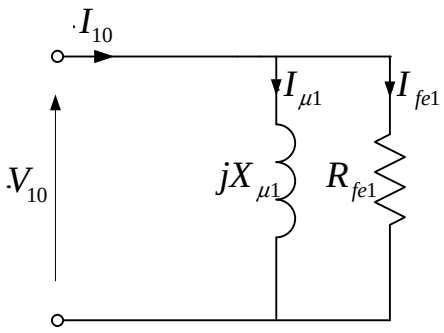

Fig.4 Equivalent circuit as “seen” by the primary when the secondary is unloaded.

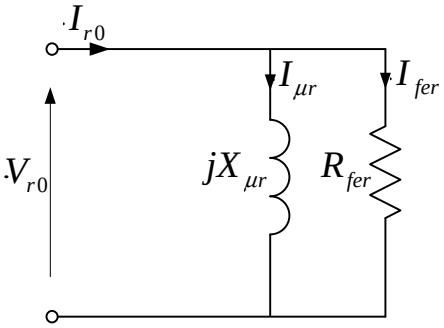

Fig.5 Equivalent circuit as “seen” by the compensation winding when the secondary is unloaded.

The two laboratory measurement diagrams adopted for the open circuit tests are shown in Figs. 6 and 7, respectively.

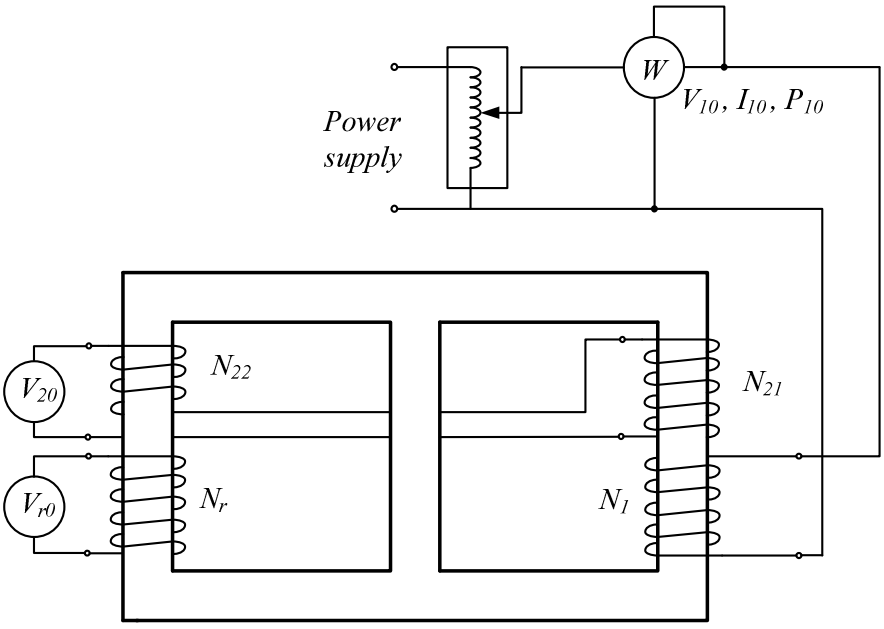

Fig.6 Electric scheme adopted for the open circuit test when the supply is on the primary.

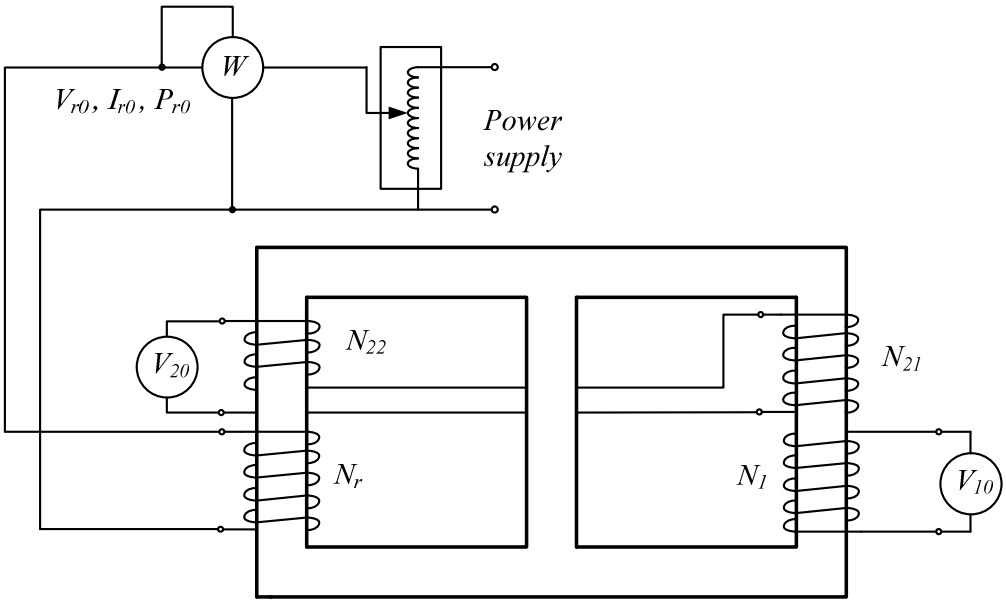

Fig.7 Electric scheme adopted for the open circuit test when the supply is on the compensation winding.

3.2 Short-circuit tests

In order to compute the elements of the series equivalent circuit, three short-circuit tests were performed, each time with two short-circuited windings and the third winding supplied with reduced voltage.

Since under these conditions the derived elements can be ignored, only the series parameters needed to be evaluated.

The first test was performed with supply on the primary allowing the computation of Z' as seen at the terminals of the supply source. With reference to Fig. 8, the following relations can be written:

$$V_{1cc} = Z_{1cc} I_{1cc} + E_1$$

$$E_2 + Z_{2cc} I_2 = 0$$

$$E_r + Z_{rcc} I_r = 0$$

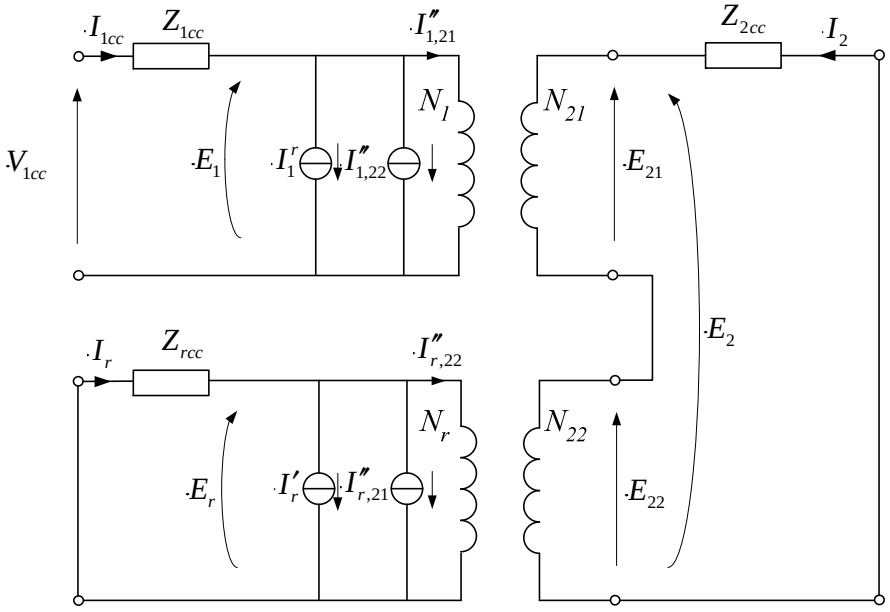

Fig.8 Equivalent circuit with both the compensation winding and secondary short-circuited.

Since:

$$E_1 = \frac{N_1}{N_{12}} E_2 - \frac{N_1 N_{22}}{N_{21} N_r} E_r$$

it is:

$$V_{1cc} = Z_{1cc} I_{1cc} - \frac{N_1}{N_{21}} Z_{2cc} I_2 + \frac{N_1 N_{22}}{N_{21} N_r} Z_{rcc} I_r \qquad (4)$$

As concerns currents, on the basis of coil ratios the following relations can be written:

$$I_r = k_{r1} I_{1cc} + k_{r,21} I_2 + k_{r,22} I_2$$
$$I_2 = k_{21,1} I_{1cc} + k_{21,r} I_r$$

The solutions of the above system are:

$$I_r = \frac{k_{r1} + k_{r,21} k_{21,1} + k_{r,22} k_{21,1}}{1 - k_{r,21} k_{21,r} - k_{r,22} k_{21,r}} I_{1cc}$$
$$I_2 = \frac{k_{21,1} + k_{21,r} k_{r1}}{1 - k_{r,21} k_{21,r} - k_{r,22} k_{21,r}} I_{1cc}$$

Z' can be computed by substituting these two relations in equation (4) and then dividing by I_{1cc}:

$$Z' = Z_{1cc} - \frac{N_1}{N_{21}} \frac{k_{21,1} + k_{21,r} k_{r1}}{1 - k_{r,21} k_{21,r} - k_{r,22} k_{21,r}} Z_{2cc} +$$

$$\frac{N_1 N_{22}}{N_{21} N_r} \frac{k_{r1} + k_{r,21} k_{21,1} + k_{r,22} k_{21,1}}{1 - k_{r,21} k_{21,r} - k_{r,22} k_{21,r}} Z_{rcc} \qquad (5)$$

By substituting to all k_{ij} quantities their expressions, the (5) relation becomes:

$$Z' = Z_{1cc} + \left(\frac{N_1}{N_{21}}\right)^2 Z_{2cc} + \left(\frac{N_1 N_{22}}{N_{21} N_r}\right)^2 Z_{rcc} \qquad (6)$$

Relation (6) supplies the impedance as seen at the primary terminations when the terminals of the other windings are short-circuited. The measurement circuit for this condition is shown in Fig. 9.

An iteration of the above procedure allows a computation of the impedances as seen at the terminals of the other two windings:

$$Z'' = Z_{2cc} + \left(\frac{N_{21}}{N_1}\right)^2 Z_{1cc} + \left(\frac{N_{22}}{N_r}\right)^2 Z_{rcc} \qquad (7)$$

$$Z^r = Z_{rcc} + \left(\frac{N_r}{N_{22}}\right)^2 Z_{2cc} + \left(\frac{N_r N_{21}}{N_{22} N_1}\right)^2 Z_{1cc} \qquad (8)$$

where Z'' is the impedance as seen at the secondary terminals when both the primary and compensation windings are short-circuited, and Z^r is the impedance as seen at the compensation winding terminals when both the primary and secondary windings are short-circuited. These conditions are shown in Figs. 10 and 11, respectively.

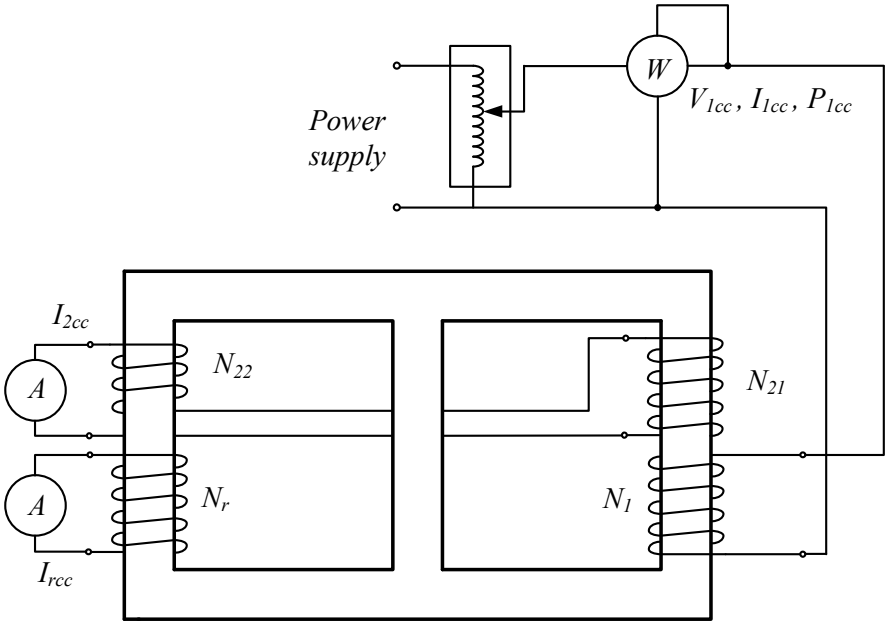

Fig.9 Short-circuit test when the supply is on the primary terminals.

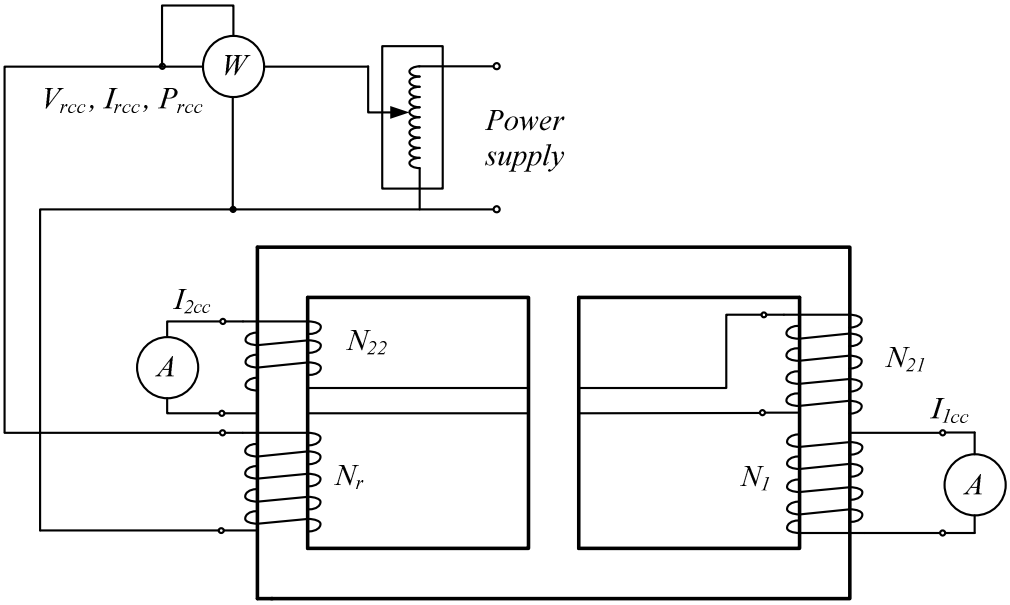

Fig.10 Short-circuit test when the supply is on the compensation winding.

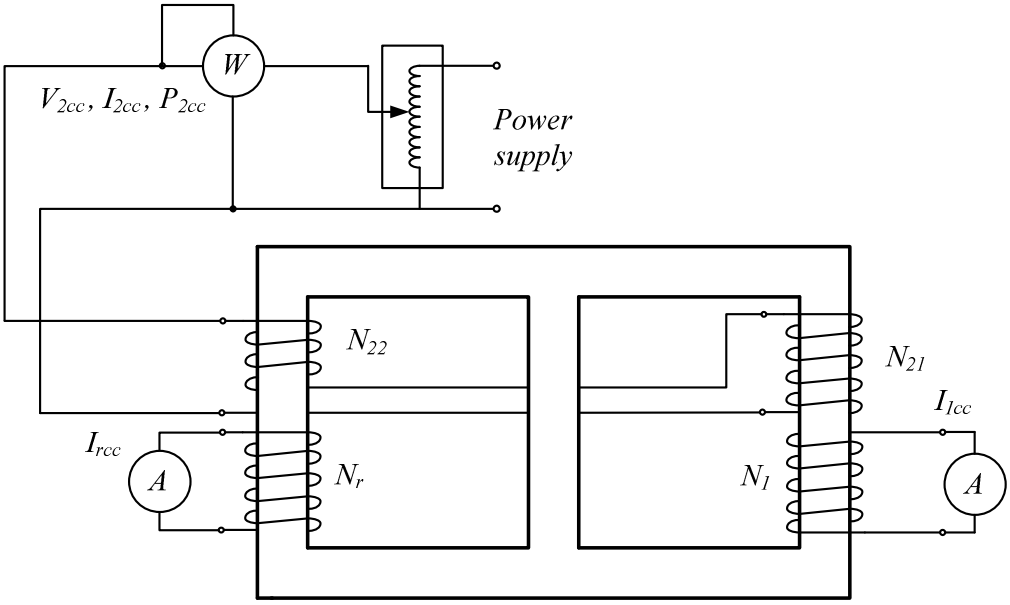

Fig.11 Short-circuit test when the supply is on the secondary.

Equations (6), (7) and (8) allow an evaluation of series impedances in the equivalent circuit.

4 Experimental performances of the machine prototype

Once the non-ideal parameters of the electrical machine were evaluated, subsequent laboratory tests were performed in order to investigate the operating performance of the prototype described in the following.

The magnetic core had the following dimensions:

- Leg cross section: 60 x 60 mm.
- Yoke cross section: 60 x 60 mm.
- Leg height: 160 mm.
- Yoke length: 240 mm.

The windings had the following coil numbers:

- N_{22}=63 coils.

- N_r =222 coils.
- N_{21}=247 coils.
- N_1 =247 coils.

All windings were made of copper conductors with a 5 mm^2 cross-section. The maximum allowed voltage and current for each winding were 400V and 50A, respectively, and the rated power of the machine was 5 kVA.

Experimental tests were performed off-line using two variacs, the former supplying the system and the latter the balancing winding. The supply variac simulated slow voltage changes due to both load variations and other events in the primary supply network, as well as quick voltage changes due to sags and swells.

The balancing variac, which in the off-line tests replaced and simulated the inverter of Fig. 1, was manually managed in order to restore the secondary voltage to its rated value under all working conditions.

Experimental tests allowed the investigation of the following case studies:

- Changes in primary supply voltage.
- Changes in secondary voltage caused by load changes.
- Sag compensation.
- Swell reduction.

The measurement system is shown in Fig. 12, while Table 1 shows the results of the experimental tests simulating all different working conditions of the system, including slow voltage changes and such sudden voltage disturbances as sags and swells. The initial experimental tests were arranged in such a way to simulate secondary voltage changes due to load changes. Table 1 shows that in these cases voltage recovery required very low compensation power, within 2.3% - 3.4% of the load power. Subsequent tests dealt with quick disturbances such as sags and swells. In these cases, a quite higher, 35.5% compensation power was needed to recover a 30% sag. Simulated swells reached maximum values of 30% and required compensation power within 2.2% and 16.3% of the load power.

It is convenient here to recall that to achieve swell compensation the terminations of compensation windings need to be inverted.

If the maximum power established for the compensation winding is 20÷25% of the power unit, the prototype can compensate all load changes, as well as sags as low as -20% and swells up to +25%. In other words, this means that to completely counteract the above disturbances a compensation inverter having 20% the system rated power is required.

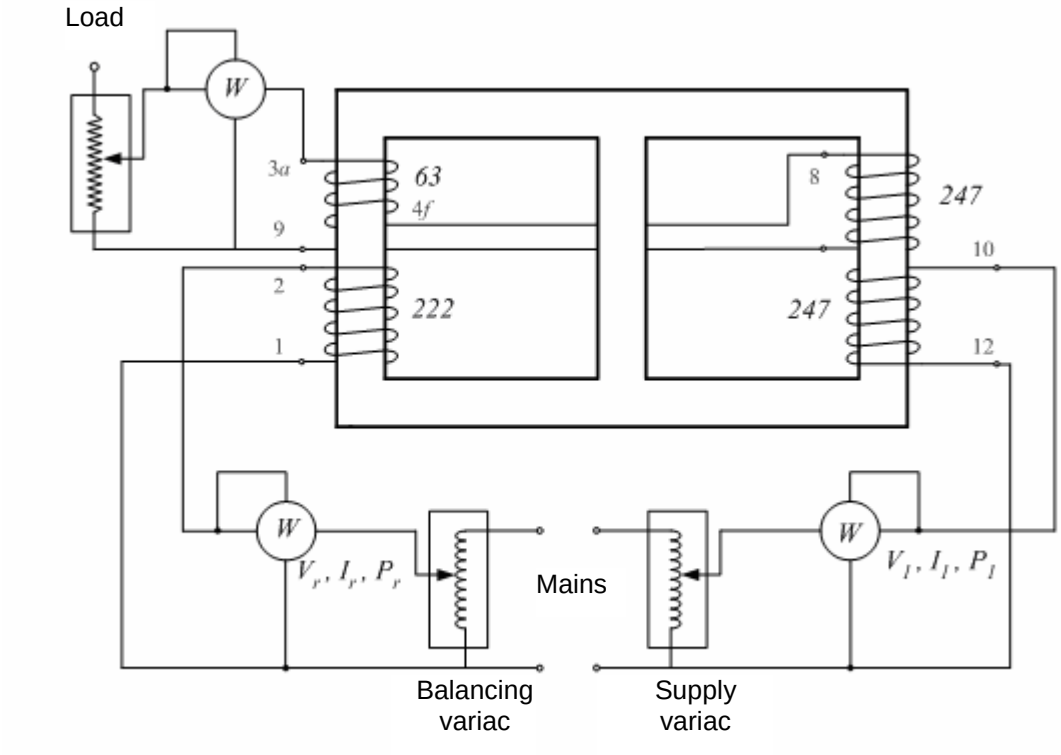

Fig.12 Measurement scheme of the laboratory tests.

Table 1 Results of the experimental tests.

	V_1 (V)	I_1 (A)	P_1 (W)	V_2 (V)	I_2 (A)	P_2 (V)	V_r (V)	I_r (A)	P_r (W)	% V_{1n}	P_r %	η
Unloaded	180.2	0.22	14.2	180.3	0.00	0.0	0.8	0.09	0.1	100.0	-	-
Load changes	180.0	4.09	730.0	180.0	3.98	716.0	26.6	0.50	13.6	100.0	1.9	0.963
	180.3	4.42	792.0	180.0	4.32	776.0	27.7	0.53	14.2	100.0	1.9	0.963
	180.3	4.65	833.0	180.0	4.54	817.0	30.7	0.56	16.5	100.0	2.0	0.962
	180.0	5.14	921.0	180.0	5.05	908.0	34.9	0.62	20.7	100.0	2.3	0.964
	180.0	5.63	1008.0	180.0	5.54	994.0	39.5	0.67	25.5	100.0	2.6	0.962
	180.0	6.05	1078.0	180.0	5.91	1064.0	43.2	0.71	29.7	100.0	2.8	0.961
Sags	180.3	5.10	913.0	180.0	5.00	898.0	30.5	0.60	17.9	100.0	2.0	0.965
	171.1	5.14	871.0	180.2	5.00	901.0	121.8	0.78	76.9	95.1	8.5	0.951
	162.4	5.52	931.0	180.0	5.00	898.0	210.1	2.27	148.0	90.2	16.5	0.917
Swells	189.5	5.09	959.0	180.0	5.00	899.0	50.6	0.55	-27.4	105.3	3.1	0.965
	198.5	5.07	999.0	180.0	5.00	899.0	134.4	0.50	-69.9	110.1	7.7	0.968
	207.8	5.06	1047.0	180.2	5.01	901.0	220.8	0.50	-101.6	115.4	11.3	0.953

5 Response time of the system

Further experimental investigations were carried out in order to evaluate the response time of the proposed voltage controller. Among the different time values involved, including those of the acquisition system (micro electronics), actuator device (power electronics), microprocessor (computation) and special transformer (magnetization), only the last is to be taken into account since it is in the order of *ms* with the others being only μs. Therefore experimental tests were performed on the machine only in order to establish the time necessary for magnetization changes to appear in the transformer core.

The experimental examination reported in the following was targeted at evaluating the response time of the transformer from the first occurrence of a sag until voltage could be restored to its rated value. During this time interval, the voltage transient was recorded by means of an oscilloscope.

The sag was generated by placing a series resistance upstream the transformer as shown in Fig. 13.

When the contactor is closed the following condition is obtained:

Vp=Vp'=1 p.u.

The experimental test examined an open operation of the contactor causing a 20% sag (Vp=0.8 p.u.). The starting time of the sag was established by means of a programmable electronic device adequately coordinated with an oscilloscope, as shown in Fig. 14.

The results of the experiment are reported in Figs. 15 and 16, which show that the sag was promptly recovered by the control system.

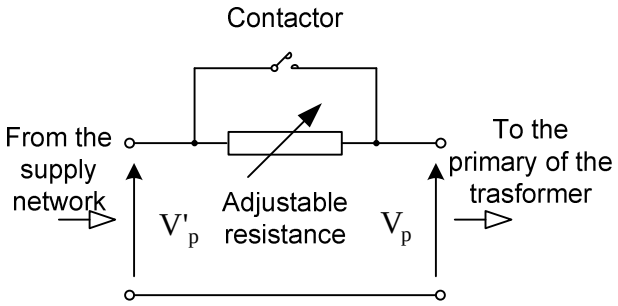

Fig.13 Layout of the power device used to generate a sag.

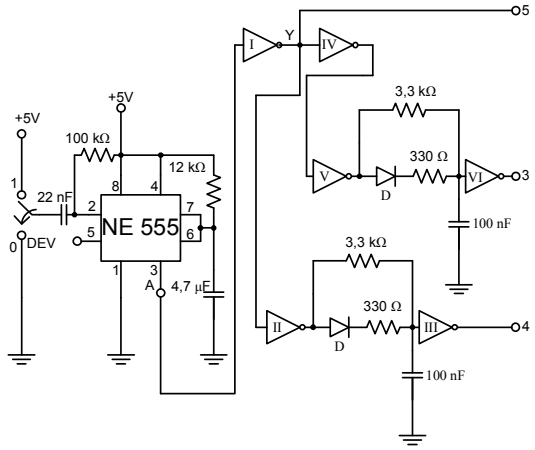

Fig.14 Electronic circuit used to control the starting point and duration of the sag.

The system response time can be accurately evaluated from Fig. 16 showing an enlargement of the previous figure in correspondence of the recorded transient, whose starting time is 10 *ms*. The time unit adopted in Fig. 16 is *ms*. Fig. 16 also shows that the transient response took place in less than 1 *ms*, a much lower interval than the recovery time usually required by the most sensitive preferential and privileged loads [18].

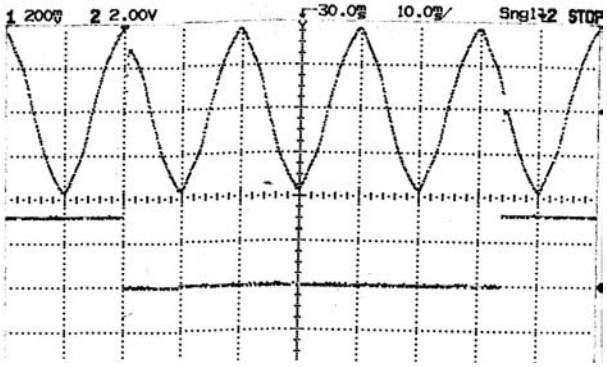

Fig.15 Recording of a transient concerning a sag generation and subsequent voltage recovery.

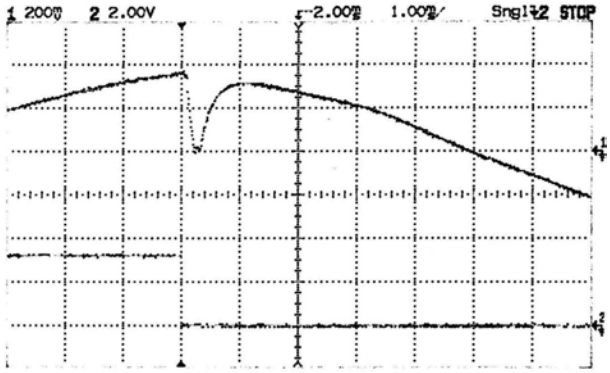

Fig.16 Enlargement of the transient shown in Fig. 15.

For this reason, the delay introduced by the core magnetization can be widely accepted.

6 Prospective research

Nowadays electrical systems and apparatuses are more and more targeted towards very high automation levels, which are usually reached by an ever-growing number of electronic devices such as PLCs (Programmable Logic Controller), microprocessors, microcontrollers, sensors, transducers, digital protections and so on. Though allowing complex operations without the intervention or supervision of an operator, these devices are very sensitive to a number of disturbances – such as long, medium and micro interruptions, voltage sags and swells, harmonic pollution – which can in turn cause serious inconveniences often followed by heavy system damages and even substantial economic losses. It is therefore evident that while on the one hand quality standards in industrial production have been constantly raised introducing automation to eliminate subjective manual intervention, on the other hand this growingly automated scenario involves huge risks arising from the high vulnerability of the system, thus vanifying all efforts towards automation. For all these reasons, power quality and reliability of the electrical supply must be extremely high [16]. With this consideration in mind, prospective research aiming at improving the proposed voltage controller will mainly attempt to develop a real time control able to condition not only the RMS value but also instantaneous voltage values. This objective may be achieved on-line with a faster control of the magnetic flux linked to the secondary winding of the special transformer. The final aim will be to obtain a perfect, real-time controlled waveform of the secondary voltage.

7 Conclusions

Nowadays changes of paramount importance are taking place in power distribution due to both the remarkable penetration of distributed generation and the growing liberalization of the energy market.

The present, mainly passive distribution networks will need to change into active in order to allow bi-directional power flows and turn customers into energy buyers and sellers at the same time.

This scenario will require greater automation in system management, therefore the herein proposed voltage conditioner, joining the advantages of a transformer – robustness, reliability, efficiency, low maintenance, etc. – with the capabilities of power electronics and digital technologies, might effectively be used to control voltage profiles in distribution systems as well as for high-technology, industrial applications.

References

[1] F. Muzi, A New Configuration for Uninterruptible Distribution Systems, *IEEE-PES 1999 Winter Meeting*, January 31 – February 4, 1999, New York, USA.

[2] G. Fazio, V. Lauropoli, F. Muzi, G. Sacerdoti, Variable-window Algorithm for Ultra-high-Speed Distance Protection, *IEEE Transactions on Power Delivery*, Vol.18, No.2, April 2003.

[3] C. Bartoletti, M. Desiderio, D. Di Carlo, G. Fazio, F. Muzi, G. Sacerdoti, F. Salvatori, Vibro-acoustic Techniques to Diagnose Power Transformers, *IEEE Transactions on Power Delivery*, Vol. 19, No.1 January 2004.

[4] G. C. Lee, M. M. Albu, G. T. Heydt, A Power Quality Index Based on Equipment Sensitivity, Cost, and Network Vulnerability, *IEEE Transactions on Power Delivery*, Vol.19, No.3, 2004.

[5] F. Muzi, An Alternative FMECA Procedure to Design Distribution System Reliability, *WSEAS Transactions on Power Systems*, Issue 11, Vol.1, November 2006.

[6] A. M. Youssef, T. K. Abdel-Galil, E. F. El-Saadany, M. M. Salama, Disturbance Classification Utilizing Dynamic Time Warping Classifier, *IEEE Transactions on Power Delivery*, Vol.19, No. 1, 2004.

[7] A. M. Stankovi´c, H. Levi-Ari, M. M. Peri˘si´c, Analysis and Implementation of Model-based Linear Estimation of Dynamic Phasors, *IEEE Transactions on Power Systems*, 2004, 19, (4), pp. 1903–1910.

[8] M. Karimi, H. Mokhtari, M. R. Iravani, Wavelet Based on-line Disturbance Detection for Power Quality Applications, *IEEE Transactions on Power Delivery*, vol. 15, no. 4, pp. 1212–1220, 2000.

[9] M. H. J. Bollen, What is Power Quality?, *Electric Power Systems Research*, Vol.66, No.1, 2003, pp. 5-14.

[10] C. Hochgraf, R. H. Lasseter, Statcom Controls for Operation with Unbalanced Voltages, *IEEE Transactions on Power Delivery*, Vol.13, No.2, April 1998.

[11] M. J. Grady, W. M. Samotyj, A. H. Noyola, Survey of Active Power Line Conditioning Methodologies, *IEEE Transactions on power Delivery*, vol. 5, no. 3, pp. 1536–1542, July 1990.

[12] R. El Shatshat, M. Kazerani, Modular Active Power-Line Conditioner, *IEEE Transactions on Power Delivery*, Vol.16, No.4, October 2001.

[13] M. H. J. Bollen, *Understanding Power Quality Problems,* IEEE Press Series on Power Engineering, New York, 2000.

[14] Z. L. Gaing, Wavelet-based neural network for power disturbance recognition and classification, *IEEE Transactions on Power Delivery*, Vol.19, No.4, pp.1560–1568, 2004.

[15] T. A. Short, A. Mansoor, W. A. Sunderman, Site Variation and Prediction of Power Quality, *IEEE Transactions on Power Delivery*, Vol.18, No.4, October 2003 1369.

[16] C. Bartoletti, G. Fazio, F. Muzi, S. Ricci, G. Sacerdoti - Diagnostics of Electric Power Components: An Improvement on Signal Discrimination, *WSEAS Transactions on Circuits and Systems*, Issue 7, Vol.4, July 2005.

[17] D. Lascu, M. Lascu, M. Tanase, I. Lie, A Novel Step-up Converter and its Application, *WSEAS Transactions on Circuits and Systems*, Issue 8, Vol.5, August 2006.

[18] F. Muzi, C. Buccione, S. Mautone, A New Architecture for Systems Supplying Essential Loads in the Italian High-Speed Railway (HSR), *WSEAS Transactions on Circuits and Systems*, Issue 8, Vol.5, August 2006.